Spatial Functional Characteristics of East Asian Patients With Occult Macular Dystrophy (Miyake Disease); EAOMD Report No. 2

LIZHU YANG, KWANGSIC JOO, KAZUSHIGE TSUNODA, MINEO KONDO, YU FUJINAMI-YOKOKAWA, GAVIN ARNO, NIKOLAS PONTIKOS, XIAO LIU, NATSUKO NAKAMURA, TOSHIHIDE KURIHARA, KAZUO TSUBOTA, TAKESHI IWATA, HUI LI, XUAN ZOU, SHIJING WU, ZIXI SUN, SEONG JOON AHN, MIN SEOK KIM, YONG SEOK MUN, KYU HYUNG PARK, ANTHONY G. ROBSON, YOZO MIYAKE, SE JOON WOO, RUIFANG SUI, AND KAORU FUJINAMI, FOR THE EAST ASIA INHERITED RETINAL DISEASE SOCIETY STUDY GROUP

• PURPOSE: To describe the functional phenotypic features of East Asian patients with *RP1L1*-associated occult macular dystrophy (ie, Miyake disease).

• DESIGN: An international multicenter retrospective cohort study.

• METHODS: Twenty-eight participants (53 eyes) with Miyake disease were enrolled at 3 centers (in Japan, China, and South Korea). Ophthalmologic examinations including spectral-domain optical coherence tomography (SDOCT) and multifocal electroretinogram (mfERG) were performed. Patients were classified into 3 functional groups based on mfERG: Group 1, paracentral dysfunction with relatively preserved central/peripheral function; Group 2, homogeneous central dysfunction with preserved peripheral function; and Group 3, widespread dysfunction over the recorded area. Three functional phenotypes were compared in clinical parameters and SDOCT morphologic classification (severe phenotype, blurred/flat ellipsoid zone and absence of the interdigitation zone; mild phenotype, preserved ellipsoid zone).

• RESULTS: There were 8 eyes in Group 1, 40 eyes in Group 2, and 5 eyes in Group 3. The patients in Group 1 showed significantly later onset ($P = .005$) and shorter disease duration ($P = .002$), compared with those in Group 2. All 8 eyes in Group 1 showed the mild morphologic phenotype, while 43 of 45 eyes in Groups 2 and 3 presented the severe phenotype, which identified a significant association between the functional grouping and the morphologic classification ($P < .001$).

• CONCLUSIONS: A spectrum of functional phenotypes of Miyake disease was first documented with identification of 3 functional subtypes. Patients with paracentral dysfunction had the mildest phenotype, and those with homogeneous central or widespread dysfunction showed overlapping clinical findings with severe photoreceptor changes, suggesting various extents of visual impairment. (Am J Ophthalmol 2021;221:169–180.

AJO.com Supplemental Material available at AJO.com.

Accepted for publication Jul 14, 2020.

From the Department of Ophthalmology, Peking Union Medical College Hospital, Peking Union Medical College and Chinese Academy of Medical Sciences, Beijing, China (L.Y., H.L., X.Z., S.W., Z.S., R.S.); Laboratory of Visual Physiology, Division of Vision Research, National Institute of Sensory Organs, National Hospital Organization Tokyo Medical Center, Tokyo, Japan (L.Y., K.T., Y.F.-Y., G.A., N.P., X.L., N.N., Y.M., K.F.); Department of Ophthalmology, Keio University School of Medicine, Tokyo, Japan (L.Y., X.L., T.K., K.T., K.F.); Department of Ophthalmology, Seoul National University Bundang Hospital, Seoul National University College of Medicine, Seongnam, South Korea (K.J. M.S.K., Y.S.M., K.H.P., S.J.W.); Department of Ophthalmology, Mie University Graduate School of Medicine, Tsu, Japan (M.K.); Department of Health Policy and Management, Keio University School of Medicine, Tokyo, Japan (Y.F.-Y.); Division of Public Health, Yokokawa Clinic, Suita, Japan (Y.F.-Y.); UCL Institute of Ophthalmology, London, United Kingdom (Y.F.-Y., G.A., N.P., A.G.R., K.F.); Moorfields Eye Hospital, London, United Kingdom (G.A., N.P., A.G.R., K.F.); Department of Ophthalmology, The University of Tokyo, Tokyo, Japan (N.N.); Division of Molecular and Cellular Biology, National Institute of Sensory Organs, National Hospital Organization Tokyo Medical Center, Tokyo, Japan (T.I.); Department of Ophthalmology, Hanyang University Hospital, Hanyang University College of Medicine, Seoul, South Korea (S.J.A.); Aichi Medical University, Nagakute, Aichi, Japan (Y.M.); and Next Vision, Kobe Eye Center, Hyogo, Japan (Y.M.).

[1] Kaoru Fujinami, Kwangsic Joo, and Lizhu Yang are joint first authors.

Inquiries to Kaoru Fujinami, Laboratory of Visual Physiology, Division of Vision Research, National Institute of Sensory Organs, National Hospital Organization Tokyo Medical Center, 2-5-1 Higashigaoka, Meguro-ku, Tokyo 152-8902, JapanInquiries to Ruifang Sui, Department of Ophthalmology, Peking Union Medical College Hospital, 1 Shuai Fu Yuan, Dongcheng District, Beijing 100730, ChinaInquiries to Se Joon Woo, Department of Ophthalmology, Seoul National University College of Medicine, Seoul National University Bundang Hospital, 173-82 Gumi-ro, Bundang-gu, Seongnam-si, Gyeonggi-do 13620, South Korea; e-mails: sejoon1@snu.ac.kr; hrfsui@163.com; k.fujinami@ucl.ac.uk

OCCULT MACULAR DYSTROPHY (OMD; ONLINE Mendelian Inheritance in Man [OMIM] 613587), first described by Miyake and associates in 1989, is a type of inherited macular dystrophy characterized by progressive visual acuity loss but without visible abnormality of the fundus or fluorescein angiogram.[1–4]

In 2010, causative heterozygous variants in retinitis pigmentosa 1–like 1 gene (*RP1L1*, OMIM 608581) were

first described in 2 families with autosomal dominant OMD.[5,6] Immunohistochemistry showed the expression of *RP1L1* protein by human *RP1L1* antibody in the rod and cone photoreceptors in the macula of Cynomolgus monkeys (*Macaca fascicularis*).[3,6] *RP1L1* is assumed to be involved in the morphologic and functional maintenance of photoreceptors in interaction with *RP1* to assemble and stabilize axonemal microtubules in the connecting cilia, although the detailed function and the exact disease-causing mechanism are still uncertain owing to lack of rodent models.[3,6] In 2016, it was reported that *RP1L1*-associated OMD (ie, Miyake disease) was clinically distinct from other forms of occult maculopathy and OMD-like syndromes (also associated with a normal fundus and macular dysfunction).[7]

Electrophysiological findings are key to the diagnosis of OMD. Typical findings include a normal full-field electroretinogram (ERG) with abnormal macular function, as revealed by focal macular ERG, multifocal ERG (mfERG), or pattern ERG P50 abnormality.[1,2,8–13] Local responses from different regions of the posterior pole may be obtained with mfERG and this method is helpful to determine the spatial distribution of posterior pole dysfunction in OMD.[14,15] Previous studies reported markedly reduced mfERG responses at the fovea,[8–10,16] but in relatively few subjects and with limited investigations using spectral-domain optical coherence tomography (SDOCT). More importantly, the recruitment of specific patients focusing on Miyake disease was not available owing to a lack of molecular genetic diagnosis, which is essential to understand the underlying disease mechanism.

SDOCT provides valuable in vivo information about the microstructure of photoreceptors in OMD.[6,7,13,16–26] There are 2 microstructural subtypes of occult macular dysfunction syndrome: a classical type with both blurred ellipsoid zone (EZ) and absence of the interdigitation zone (IZ) and a nonclassical type lacking these 2 features.[4,7] Most patients with Miyake disease show classical SDOCT findings. The second group of patients generally shows a milder structural change than in Miyake disease, with local IZ absence and relatively preserved EZ.[4] In 2017, 4 patients with this subtle phenotype were reported, showing preserved visual acuity and spared central foveal photoreceptors[19]; then the clinical stages of OMD based on changes of the photoreceptor layers detected by SDOCT were published.[21] However, detailed functional assessment of Miyake disease in a large cohort including patients with various disease severities is still lacking and the spectrum of functional phenotypes has not been established.

Therefore, the purpose of this study is to determine the detailed functional characteristics of Miyake disease based on a large East Asian patient cohort. This study also provides the opportunity to investigate the variability of disease severity by assessing the spatial distribution of functional decline and to study the association between functional phenotype and morphologic phenotype.

METHODS

• **PARTICIPANTS:** This study is an international multicenter retrospective cohort study. The subjects of this study were recruited from the East Asia Occult Macular Dystrophy (EAOMD) Study cohort, which was established by 3 institutions of the East Asia Inherited Retinal Disease Society (EAIRDs; https://www.eairds.org/): the National Institute of Sensory Organs (NISO), National Hospital Organization Tokyo Medical Center, Tokyo, Japan; Peking Union Medical College Hospital (PUMCH), Beijing, China; and Seoul National University Bundang Hospital (SNUBH), Seongnam, South Korea.[4] Informed consent was obtained from all the subjects. The study protocol adhered to the tenets of the Declaration of Helsinki and was approved by the ethics committee of the participating institutions (reference numbers issued by the institutional review boards: R19-030, NISO; JS-2056, PUMCH; and B-1105/127-014, SNUBH).

The total EAOMD cohort contains 36 subjects from 21 pedigrees with a clinical diagnosis of OMD who were recruited between June 2016 and July 2017.[4] All the subjects met the diagnostic criteria of Miyake disease: (1) presence of macular dysfunction; (2) no fundus abnormalities confirmed by funduscopy; and (3) detection of a heterozygous pathogenic *RP1L1* variant.[4]

• **CLINICAL AND GENETIC INVESTIGATIONS:** The subjects underwent comprehensive ophthalmic examinations, including measurement of best-corrected visual acuity (BCVA) converted to the logarithm of the minimum angle of resolution (logMAR) unit, fundus photography/funduscopy, SDOCT, and electrophysiological assessments. The details of the applied equipment and protocols were described in a previous study.[4]

According to previous studies, 2 subtypes of SDOCT morphologic phenotype were applied to describe the structural changes: (1) severe phenotype (denoted as a classical phenotype compatible to stage IIa, IIb, IIIa, IIIb), showing both blurred/flat EZ and absence of IZ; and (2) mild phenotype (denoted as subtle morphologic changes compatible to stage Ia, Ib), defined as minimum/local blurring of EZ and local absence of IZ.[4,21]

Blood samples of the subjects were collected for genetic screening in the 3 institutes. Whole-exome sequencing with targeted analysis,[4,7,27] next-generation sequencing with targeted capture panel,[28–30] and direct sequencing[18] were performed in each institute, according to published protocols.

All clinical information and selected genetic data were uploaded to the shared database. Data quality and

conclusive diagnoses were confirmed by all 3 corresponding authors (S.J.W., R.S., K.F.).

• **RECORDINGS AND ANALYSES OF MULTIFOCAL ELECTRORETINOGRAM DATA:** The mfERGs were recorded with different recording systems in the 3 institutes. The Visual Evoked Response Imaging System (VERIS Clinic 5.0.9; Electro-Diagnostic Imaging, San Mateo, California, USA) was used with a 61-hexagon stimulus element (5 eccentric rings) in NISO.[9,17,19] VERIS (Clinic 6.0) was used with a 103-hexagon stimulus element (6 rings) in PUMCH. The RETIscan system (Roland Consult, Brandenburg, Germany) with a 61-hexagon stimulus element (5 rings), VERIS (Clinic 4.0) with a 103-hexagon stimulus element (6 rings), and UTAS (3.5.0; LKC Technologies, Gaithersburg, Maryland, USA) with a 61-hexagon stimulus element (5 rings) were used in SNUBH (Supplemental Table 1; Supplemental Material available at AJO.com). All mfERG recording procedures and protocols incorporated the international standard of the International Society for Clinical Electrophysiology of Vision (ISCEV).[14]

The peak time (ms) and response density (nV/deg^2) of the mfERG P1 component associated with the central hexagon (ring 1; R1) and eccentric areas (rings 2-5 or 2-6; R2-5 or 2-6) were measured. The mean response density for each eccentric ring was calculated as the sum of the responses divided by the total area of the hexagons within each ring as shown in Supplemental Figure 1 (Supplemental Material available at AJO.com).[14] Ring ratios were calculated based on the amplitude of the P1 component divided by the amplitude of the most peripheral ring (R5 for the 61-hexagon protocol, R6 for the 103-hexagon protocol); that is, R1/R5, R2/R5, R3/R5, and R4/R5 or R1/R6, R2/R6, R3/R6, R4/R5, and R5/R6. Normative range data were referred to in each recording condition: the VERIS 61-hexagon protocol, RETIscan 61-hexagon protocol, and VERIS 103-hexagon protocol. The most peripheral ring (R5 or R6) was assessed compared with the available normative range. Ring ratios (R1/R5) of the eyes recorded with 61-hexagon protocols were also compared among the 3 different severity grades of BCVA (favorable, ≤0.3 in the logMAR unit; intermediate, >0.3 but <1.0 in the logMAR unit; and severe, ≥1.0 in the logMAR unit).

• **MULTIFOCAL ELECTRORETINOGRAM FUNCTIONAL GROUPING:** Three functional groups were defined based on the mfERG ring ratios and P1 amplitudes in order to describe the spatial extent of functional decline. All eyes were classified into 1 of 3 groups: Group 1, paracentral dysfunction (attenuation of R2 responses) with relatively preserved central (R1) and peripheral function (R5/6); Group 2, homogeneous central/paracentral dysfunction (attenuation of responses in R1 and R2) with preserved peripheral function (R5/6); Group 3, widespread dysfunction over the whole area tested (abnormal responses in R1-R5/6). The classification of mfERG groups was performed by 2 investigators (L.Y., K.F.) masked to the structural and clinical features of the patients at the time of the review. If classifications by the 2 investigators differed, further reviews were performed and discussed to enable a consensus. Ring ratios recorded with the 61-hexagon protocol were compared between functional groups.

• **CLINICAL PARAMETERS AND MORPHOLOGIC PHENOTYPES FOR MULTIFOCAL ELECTRORETINOGRAM FUNCTIONAL GROUPS:** To characterize the functional phenotypes, mfERG functional groups were compared in terms of clinical parameters: age, age at onset, duration of disease, and BCVA. An association between functional grouping and SDOCT morphologic classification (severe phenotype/mild phenotype) was also investigated.

• **STATISTICAL ANALYSES:** Statistical analyses were performed using SPSS Statistics (Version 24, Statistical Package for the Social Sciences; IBM Corp, Armonk, New York, USA). The comparison analyses for the clinical parameters between the functional groups were performed with the Kruskal-Wallis test. One eye of each subject was randomly selected with the online Random Integer Generator (https://www.random.org/integers/) to perform the analysis for age, age at onset, and duration of disease. The Goodman-Kruskal gamma, a measure of association for ordered categories ranging between −1 and +1 for perfect negative and positive association, respectively, was calculated to measure the association between functional grouping and SDOCT morphologic classification.[31] *P* values less than .05 were considered statistically significant.

RESULTS

• **PARTICIPANTS, DEMOGRAPHICS, AND CLINICAL AND GENETIC FINDINGS:** In total, 53 eyes of 28 patients with available mfERGs from 18 families were recruited from the EAOMD cohort. There were 17 male (17/28, 60.7%) and 11 female patients (11/28, 39.3%). The detailed clinical and genetic information is summarized in Table 1. There were 18 patients from 10 families recruited at NISO, 5 patients from 3 families at PUMCH, and 5 patients from 5 families at SNUBH.

The median age at the latest examination was 48.0 (range, 12.0-86.0) years. The median age at onset was 35.0 (range, 6.0-73.0) years. The median disease duration (between the age at onset and the latest examination) was 8.5 (range, 0-36.0) years. The median BCVA was 0.52 (range, −0.08 to 1.22) in logMAR units. All patients showed normal full-field ERGs. There were 43 eyes (43/53, 81.1%) from 23 subjects showing the severe phenotype and 10 eyes (10/53, 18.9%) from 5 subjects showing the mild phenotype evident on SDOCT.

TABLE 1. Clinical and Genetic Features of 28 Subjects With Occult Macular Dystrophy Harboring Heterozygous Pathogenic *RP1L1* Variants (Miyake Disease)

Patient No.	Patient ID[a]	Inheritance	Sex	Age[b] (y)	Onset[b]	Chief Complaint	BCVA (logMAR)		SDOCT Phenotype[c]	SDOCT Stage		*RP1L1* Variant[d]
							OD	OS		OD	OS	
1	1-II:1	Unknown	F	35	25	Reduced VA/photophobia	0.52	0.52	Severe	IIb	IIb	c.133C>T, p.Arg45Trp
2	2-III:2	AD	F	17	6	Reduced VA	0.70	0.52	Severe	IIb	IIb	c.133C>T, p.Arg45Trp
3	2-II:2	AD	F	48	40	Reduced VA/photophobia	1.05	0.52	Severe	IIb	IIb	c.133C>T, p.Arg45Trp
4	3-III:1	AD	F	19	11	Reduced VA	0.82	0.82	Severe	IIb	IIb	c.133C>T, p.Arg45Trp
5	3-II:1	AD	F	54	37	Reduced VA/photophobia	1.00	0.82	Severe	IIb	IIb	c.133C>T, p.Arg45Trp
6	3-II:3	AD	F	48	48	No symptom	−0.08	−0.08	Mild	Ib	Ib	c.133C>T, p.Arg45Trp
7	4-III:2	AD	M	12	8	Reduced VA	0.60	0.60	Severe	IIb	IIb	c.133C>T, p.Arg45Trp
8	4-II:4	AD	M	43	13	Reduced VA	0.82	0.82	Severe	IIb	IIb	c.133C>T, p.Arg45Trp
9	5-II:1	AD	M	31	23	Reduced VA	0.70	0.70	Severe	IIb	IIb	c.133C>T, p.Arg45Trp
10	8-III:1	AD	M	24	12	Reduced VA	0.52	0.52	Severe	IIb	IIb	c.133C>T, p.Arg45Trp
11	9-II:2	Unknown	M	45	14	Reduced VA	1.22	1.10	Severe	IIIa	IIIa	c.133C>T, p.Arg45Trp
12	10-II:2	AD	M	24	24	Poor VA	0.52	0.70	Severe	IIa	IIa	c.133C>T, p.Arg45Trp
13	11-II:1	Unknown	M	73	73	No symptom	0.30	0.00	Mild	Ib	Ib	c.133C>T, p.Arg45Trp
14	12-II:1	Unknown	M	52	47	Reduced VA/photophobia	0.30	0.40	Severe	IIa	IIa	c.3581C>T, p.Thr1194Met/c.3587C>T, p.Thr1196Ire (complex)
15	13-II:1	AD	M	30	25	Reduced VA	0.60	0.60	Severe	IIb	IIb	*c.3593C>T, p.Ser1198Phe*
16	13-I:1	AD	M	54	54	No symptom	0.05	0.22	Mild	Ib	Ib	*c.3593C>T, p.Ser1198Phe*
17	14-II:2	AD	M	58	40	Reduced VA	0.70	0.70	Severe	IIb	IIb	c.3596C>G, p.Ser1199Cys
18	14-I:2	AD	F	86	50	Reduced VA/photophobia	0.70	0.70	Severe	IIb	IIb	c.3596C>G, p.Ser1199Cys
19	15-II:1	Unknown	M	48	39	Reduced VA/photophobia	0.30	0.30	Severe	IIb	IIb	c.3596C>G, p.Ser1199Cys
20	16-IV:3	AD	M	32	26	Reduced VA/photophobia	0.15	0.22	Severe	IIIa	IIIa	c.3596C>G, p.Ser1199Cys
21	16-III:2	AD	F	62	62	No symptom	−0.08	−0.08	Mild	Ib	Ib	c.3596C>G, p.Ser1199Cys
22	17-II:4	AD	F	63	50	Reduced VA/photophobia	0.52	0.52	Severe	IIIa	IIIa	c.3596C>G, p.Ser1199Cys
23	17-III:2	AD	M	36	13	Reduced VA/photophobia	0.22	0.40	Severe	IIb	IIb	c.3596C>G, p.Ser1199Cys
24	17-III:4	AD	M	36	33	Reduced VA	0.30	0.70	Severe	IIb	IIb	c.3596C>G, p.Ser1199Cys
25	18-II:1	Unknown	M	74	50	Reduced VA	0.82	0.82	Severe	IIIb	IIIb	c.3596C>G, p.Ser1199Cys
26	19-II:2	AD	F	73	60	Reduced VA/photophobia	0.52	0.70	Severe	IIb	IIb	c.3599G>A, p.Gly1200Asp
27	19-III:1	AD	F	50	50	Night blindness	−0.08	−0.08	Mild	Ia	Ia	c.3599G>A, p.Gly1200Asp
28	21-II:1	AD	M	51	25	Reduced VA/photophobia	0.70	0.70	Severe	IIb	IIb	c.3602T>G, p.Val1201Gly

AD = autosomal dominant; BCVA = best-corrected visual acuity; logMAR = logarithm of the minimum angle of resolution; NA = not available; Pt = patient; SDOCT = spectral-domain optical coherence tomography; VA = visual acuity.

[a]Patient IDs are the ones that have been previously published elsewhere (Fujinami et al. Clinical and Genetic Characteristics of East Asian Patients with Occult Macular Dystrophy (Miyake Disease): East Asia Occult Macular Dystrophy Studies Report Number 1.*Ophthalmology* 2019; 126(10):1432-1444).[4]

[b]Age was defined as the age when the latest examination was performed. The age at onset was defined as either the age at which visual loss was first noted by the patient or, in the "asymptomatic" patients, when an abnormal retinal finding was first detected. Three asymptomatic patients (Patients 6, 16, and 21) were detected owing to the autosomal dominant family history; 1 patient (Patient 13) was detected by routine examination to check cataract.

[c]The severe phenotype, showing both blurred/flat ellipsoid zone (EZ) and absence of interdigitation zone (IZ), was demonstrated in 23 subjects, and mild phenotype, defined as minimum/local blurring of EZ and local absence of IZ was found in 5 subjects.

[d]*RP1L1* transcript ID: NM_178857.5. Italics: One novel variant found in this East Asia Occult Macular Dystrophy study.

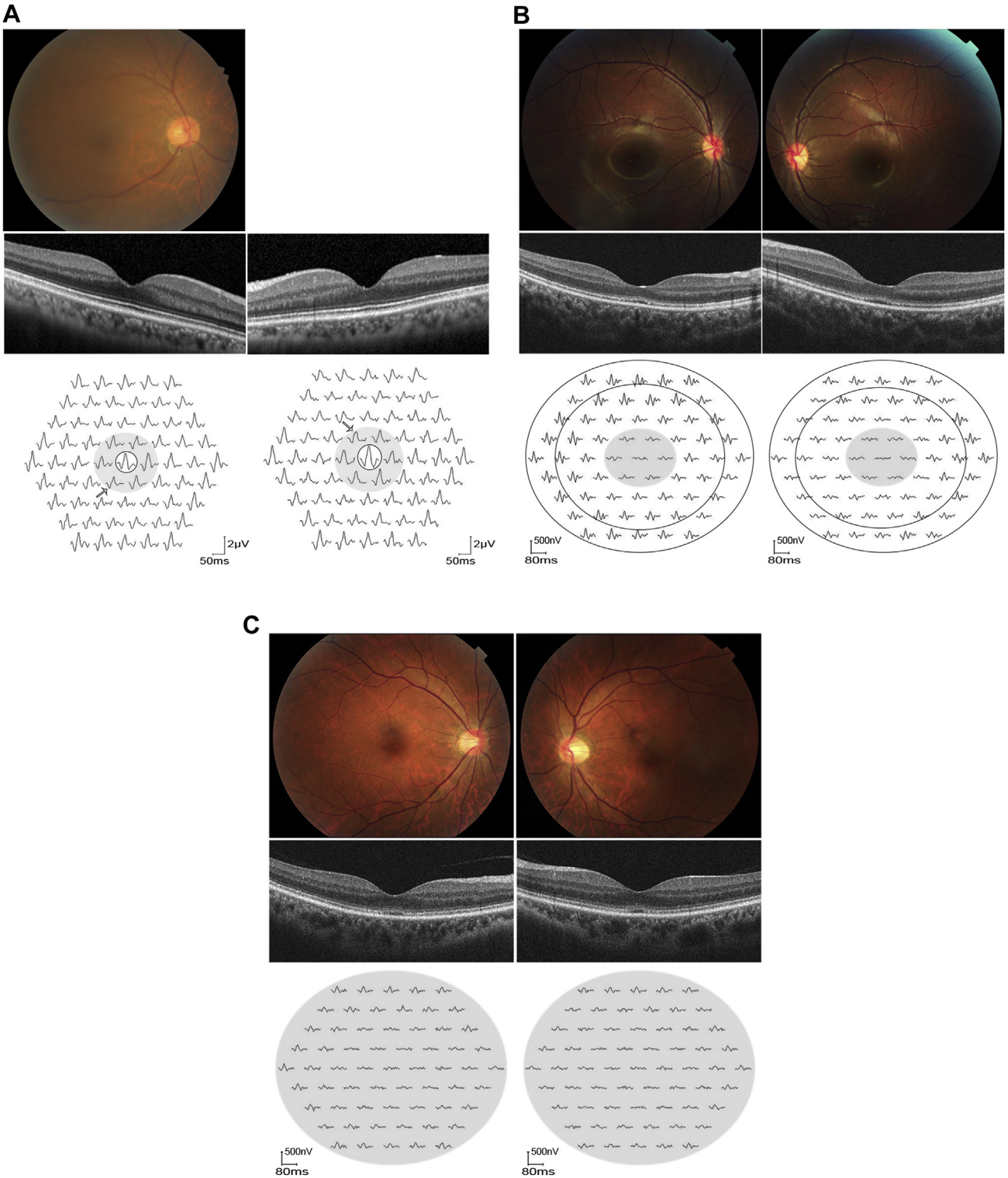

FIGURE 1. Clinical images and multifocal electroretinogram (mfERG) traces of 3 representative cases from each functional group. (A) A representative case from Group 1 (Patient 13, 11-II:1; male, 73 years, best-corrected visual acuity (BCVA) [converted to logMAR unit] 0.30/0.00 for right eye/left eye). A fundus photograph of right eye shows a normal appearance. Spectral-domain optical coherence tomographic (SDOCT) images in the fovea of the right eye and left eye demonstrate the mild phenotype with preserved ellipsoid zone (EZ) and local absence of interdigitation zone (IZ). Responses of the mfERG of right and left eyes (field view) identify relatively preserved responses of the central area (ring 1, central circle) and preserved responses of the peripheral area (ring 5) compared to the decreased responses of the paracentral area (ring 2, gray region). The arrows indicate the considerably reduced responses. (B) A representative case from Group 2 (Patient 2, 2-III:2; female, 17 years, BCVA 0.70/0.52 for right eye/left eye).

TABLE 2. Summary of Multifocal Electroretinogram Ring Ratios Recorded With the 61-Hexagon Protocol for 3 Functional Groups

Functional Group[a]	Value	Ring 1/Ring 5	Ring 2/Ring 5	Ring 3/Ring 5	Ring 4/Ring 5
Group 1	Median	4.50	2.13	1.45	1.05
	Range	(3.46-5.34)	(1.29-2.31)	(0.90-1.66)	(1.00-1.15)
Group 2	Median	1.84	1.04	0.99	1.02
	Range	(Extinguished-3.24)	(0.47-1.90)	(0.29-1.52)	(0.76-1.21)
Group 3	Median	2.16	0.82	0.69	0.95
	Range	(1.73-3.52)	(0.66-1.93)	(0.65-1.37)	(0.93-1.26)

mfERG = multifocal electroretinogram.

Ring ratios were calculated based on the amplitude (ie, response density; nV/deg^2) of the P1 component divided by the amplitude of the most peripheral ring (ring 5 for the 61-hexagon protocol).

[a]All eyes were classified into 3 functional groups based on the mfERG ring ratios and P1 amplitudes: Group 1 - paracentral dysfunction (attenuation of ring 2 responses) with relatively preserved central (ring 1) and peripheral function (ring 5); Group 2 - homogeneous central/paracentral dysfunction (attenuation of responses in ring 1 and ring 2) with preserved peripheral function (ring 5); and Group 3 - widespread dysfunction over the whole area tested (abnormal responses in rings 1-5).

Seven heterozygous pathogenic *RP1L1* variants detected in this study were within the 2 hot spots (amino acids 45 and 1196-1201), including 2 recurrent variants: c.133C>T, p.(Arg45Trp) identified in 9 families (9/18, 50.0%); and c.3596C>G, p.(Ser1199Cys) found in 5 families (5/18, 27.8%).

• **MULTIFOCAL ELECTRORETINOGRAM RING ANALYSES:** The detailed P1 amplitude density and peak time of each eccentric ring in 53 eyes of 28 subjects are described in Supplemental Table 2 (Supplemental Material available at AJO.com). Ring amplitude ratios and the grouping of mfERG phenotypes for each eye are presented in Supplemental Table 3 (Supplemental Material available at AJO.com). The median value of R1/R5, R2/R5, R3/R5, and R4/R5 with the 61-hexagon protocol was 2.04 (range, extinguished-5.34), 1.01 (range, 0.47-2.31), 0.99 (range, 0.29-1.26), and 1.01 (range, 0.76-1.26), respectively. The median value of R1/R6, R2/R6, R3/R6, R4/R6, and R5/6 with the 103-hexagon protocol was 1.34 (range, 0.62-4.38), 1.20 (range, 0.62-2.13), 1.17 (range, 0.62-1.89), 1.03 (range, 0.71-1.58), and 0.97 (range, 0.81-1.26), respectively. Median values of R1/R5 in favorable/intermediate/severe BCVA were 3.35 (range, 2.05-5.34)/1.19 (range, extinguished-2.74)/2.23 (0.64-2.76). Statistically significant difference was revealed in terms of the R1/R5 ratio between the favorable grade and the intermediate grade of BCVA ($P < .001$); a trend of difference was found between the favorable grade and the severe grade of BCVA ($P = .279$); no significant difference was found between the intermediate grade and the severe grade of BCVA ($P > .99$).

• **MULTIFOCAL ELECTRORETINOGRAM FUNCTIONAL GROUPS:** The functional groups of 53 eyes of 28 subjects are presented in Supplemental Table 3. There were 8 eyes (8/53, 15.1%) of 5 subjects in Group 1; 40 eyes (40/53, 75.5%) of 23 subjects in Group 2; and 5 eyes (5/53, 9.4%) of 3 subjects in Group 3. Clinical images and mfERG traces of 3 representative cases from each functional group are shown in Figure 1.

The ring ratios of subjects in each group recorded with the 61-hexagon protocol are summarized in Table 2 and Figure 2. Significant differences were identified between Groups 1 and 2 in R1/R5, between Groups 1 and 2 and Groups 1 and 3 in R2/R5, and between Groups 1 and 2 and Groups 1 and 3 in R3/R5. A markedly high R1/R5 ratio was noted in Group 1 (median: 4.50, range 3.46-5.34).

• **CLINICAL AND MORPHOLOGIC FINDINGS FOR MULTIFOCAL ELECTRORETINOGRAM FUNCTIONAL GROUPS:** The clinical parameters of age, age at onset, disease duration, and BCVA for the 3 functional groups are summarized in Table 3 and Figure 3. The median age of Groups 1, 2, and 3 was 54.0 (range, 48.0-71.0), 36.0 (range, 12.0-84.0), and 51.0 (range, 45.0-66.0) years, respectively. The median age at onset of symptoms of Groups 1, 2, and 3 was 54.0 (range, 48.0-71.0), 25.0 (range, 6.0-50.0), and 39.0

Fundus photographs of right eye and left eye showed a normal appearance. SDOCT images in the fovea of right eye and left eye demonstrate the severe phenotype with blurred EZ and absence of IZ. mfERG responses of right and left eyes identify homogenously reduced responses at the central and paracentral areas (ring 1 and ring 2, gray region), with preserved responses of the peripheral area (ring 5, peripheral circle). (C) A representative case from Group 3 (Patient 19, 15-II:1; male, 48 years, BCVA 0.30/0.30 for right eye/left eye). Fundus photographs of right and left eye showed normal appearance. SDOCT images in the fovea of right and left eye demonstrated the severe phenotype with blurred EZ and absence of IZ. mfERGs of right and left eye identify decreased responses of the entire recording area (rings 1-5, gray region).

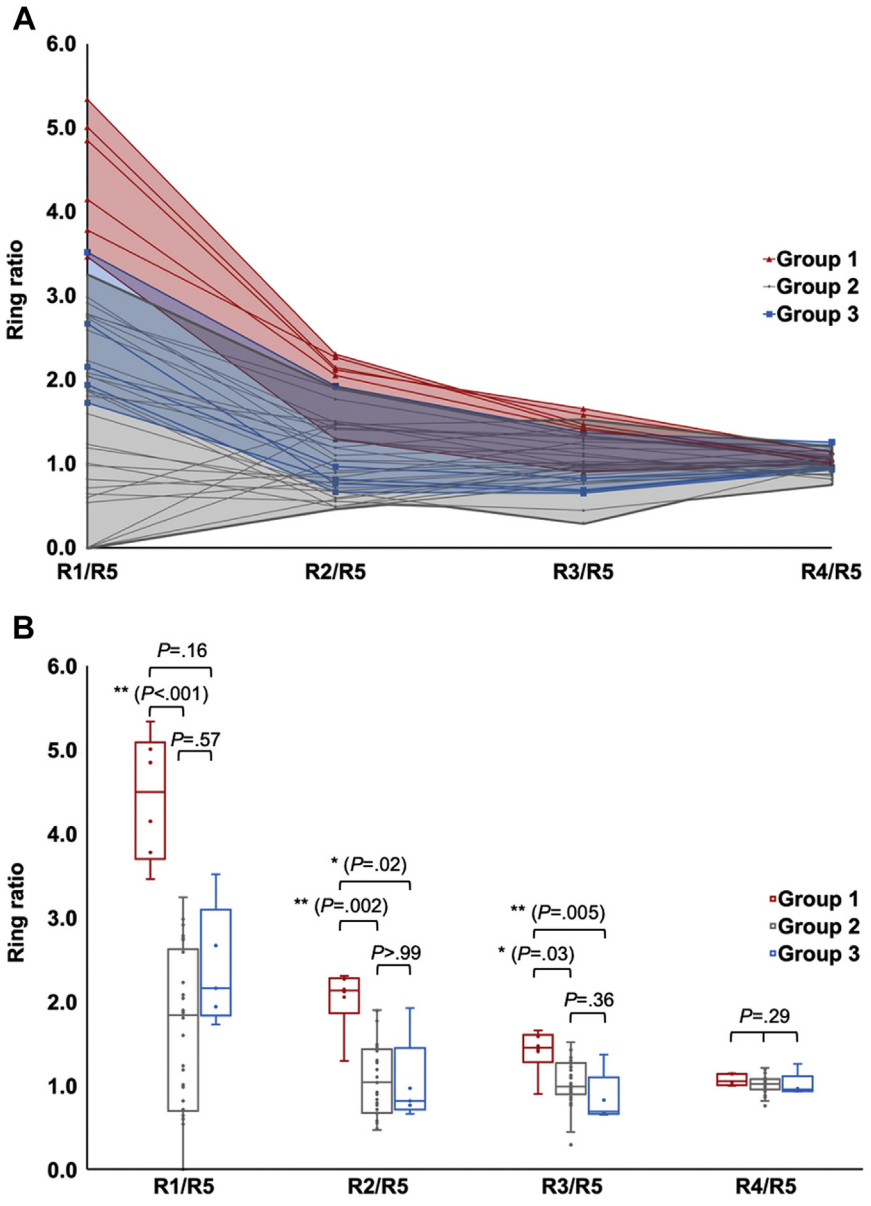

FIGURE 2. Ring ratios recorded with the 61-hexagon protocol for 3 functional groups. (A) Individual values of ring ratios of the eyes recorded with the 61-hexagon protocol. Red area: the range for ring ratios of the eyes in Group 1 (6 eyes); gray area: the range for ring ratios of Group 2 (30 eyes); blue area: the range for ring ratios of Group 3 (5 eyes). The curves of ring ratios in Group 1 have a steeper trend than those in Groups 2 and 3, while curves in Group 3 tended to be flatter than the others. R = ring. (B) Comparison between the functional groups for each ring ratio. The ends of the boxes represent the upper and lower quartiles. The middle line in the box is the median value. Maximum and minimum values are shown as the upper and lower ends of the whiskers. Statistically, significant differences were identified between Groups 1 and 2 in terms of R1/R5 (95% confidence interval [CI], 3.65 to 5.21 and 1.22 to 1.98, respectively; $P < .001$), R2/R5 (95% CI, 1.64 to 2.43 and 0.90 to 1.23, respectively; $P = .002$), and R3/R5 (95% CI, 1.13 to 1.69 and 0.93 to 1.13, respectively; $P = .03$); and between Groups 1 and 3 in R2/R5 (95% CI, 1.64 to 2.43 and 0.39 to 1.67; $P = .02$) and R3/R5 (95% CI, 1.13 to 1.69 and 0.47 to 1.22, respectively; $P = .005$). There was no significant difference in R4/R5 among the 3 groups (95% CI, 1.00 to 1.13, 0.97 to 1.05, and 0.83 to 1.18, respectively; $P = .29$).

(range, 25.0-60.0) years, respectively. The median disease duration in Groups 1, 2, and 3 was 0.0 (range, 0.0-2.0), 10.0 (range, 1.0-34.0), and 6.0 (range, 6.0-26.0), respectively. The median BCVA in Groups 1, 2, and 3 was −0.04 (range, −0.08 to 0.30), 0.65 (range, −0.08 to 1.22), and 0.52 (range, 0.30-0.70) logMAR units, respectively. Significant differences were revealed between Groups 1 and 2 in terms of the age at onset (95% confidence interval [CI], 45.2 to 68.8 and 20.3 to 34.4, respectively; $P = .005$), disease duration (95% CI, −0.7 to 1.5

TABLE 3. Clinical Parameters for 3 Functional Groups

Clinical Parameter	Value	Group 1	Group 2	Group 3
Age[a] (years)	Median	54.0	36.0	51.0
	Range	(48.0 to 71.0)	(12.0 to 84.0)	(45.0 to 66.0)
Age at onset[b] (years)	Median	54.0	25.0	39.0
	Range	(48.0 to 71.0)	(6.0 to 50.0)	(25.0 to 60.0)
Disease duration (years)	Median	0.0	10.0	6.0
	Range	(0 to 2.0)	(1.0 to 34.0)	(6.0 to 26.0)
BCVA (logMAR)	Median	−0.04	0.65	0.52
	Range	(−0.08 to 0.30)	(−0.08 to 1.22)	(0.30 to 0.70)

BCVA = best-corrected visual acuity; logMAR = logarithm of the minimum angle of resolution.

[a]Age was defined as the age when the latest examination was performed.

[b]Age at onset was defined as either the age at which visual loss was first noted by the patient or, in the "asymptomatic" patients, when an abnormal retinal finding was first detected.

and 8.9 to 18.4, respectively; $P = .002$), and BCVA (95% CI, −0.09 to 0.16 and 0.52 to 0.69, respectively; $P < .001$).

The distribution of mfERG functional grouping and SDOCT morphologic classification is described in Table 4 and Supplemental Figure 2 (Supplemental Material available at AJO.com). All 8 eyes (8/8, 100%) in Group 1 showed the mild phenotype. Thirty-eight eyes (38/40, 95.0%) in Group 2 demonstrated the severe phenotype, while 2 eyes (2/40, 5.0%) had the mild phenotype. All 5 eyes (5/5, 100%) in Group 3 showed the severe phenotype. A statistically significant association was revealed between functional group and SDOCT classification ($\gamma = 1.00$; $P < .001$).

DISCUSSION

IN THE CURRENT STUDY, THE DETAILED FUNCTIONAL FEATures of Miyake disease were determined by ring analyses of mfERGs in the largest genetically confirmed East Asian cohort, containing 53 eyes of 28 subjects.[4] Three functional phenotypes were established according to the spatial extent of mfERG abnormality. Most had central and paracentral macular dysfunction (75%), with a minority showing predominantly paracentral dysfunction (15%) or widespread dysfunction at the posterior pole (10%). These functional subtypes illustrate variable phases of disease severity of Miyake disease associated with the age at onset, visual acuity, disease duration, and morphologic abnormalities.

There are only a few studies that have described the functional features of OMD based on single-case or small cohort studies, with or without genetic diagnosis.[8–10,12,16] Piao and associates reported the amplitude (ie, response density) and peak time for the P1 component of each ring (R1-R5) in 8 Japanese patients with OMD.[9] They demonstrated that all the subjects manifested significantly decreased amplitudes of the central 2 rings (R1 and R2), with 6 (75%) showing preserved peripheral mfERG responses and 2 (25%) showing more widespread dysfunction,[9] which is mostly consistent with the current study. However, the obtained results in the current large cohort included patients with paracentral dysfunction with relatively preserved central function (5/28, 17.9%; Group 1). Therefore, a wide spectrum of functional phenotype has been found in the first large molecularly confirmed cohort of Miyake disease.

Clinical parameters for functional groups differed based on age at onset, disease duration, and BCVA. However, no difference was revealed in age among the groups. These results suggest that the age at onset is one of the key factors predicting disease severity, which was also found in other studies.[4,21]

A significant functional–morphologic association was first determined in the current study. The presence of a relatively preserved EZ line is an important sign to imply the functional subtype. Eight of 10 eyes (80%) with the mild phenotype presented maintained function in the central retina and the peripheral retina (Group 1), with 20% in Group 2. In contrast, 38 of 43 eyes (88.4%) with the severe phenotype (ie, blurred/flat EZ) demonstrated homogeneous central dysfunction (Group 2), with 11.6% in Group 3. These findings propose that the detailed assessment of the EZ line is crucial to identify the functional severity/subtype.

In the current study, distinct clinical and functional phenotypes were clarified in a subgroup of patients showing paracentral dysfunction with relatively preserved central function (Group 1). The mild phenotype is represented by a high proportion of no direct visual symptoms, late onset (in the fifth decade), favorable visual acuity, preserved EZ line, and preserved central and peripheral function, some of which were presented before.[4,7,19,21] The preceding parafoveal structural changes of OMD have been described before,[19,21] and functional decrease at the

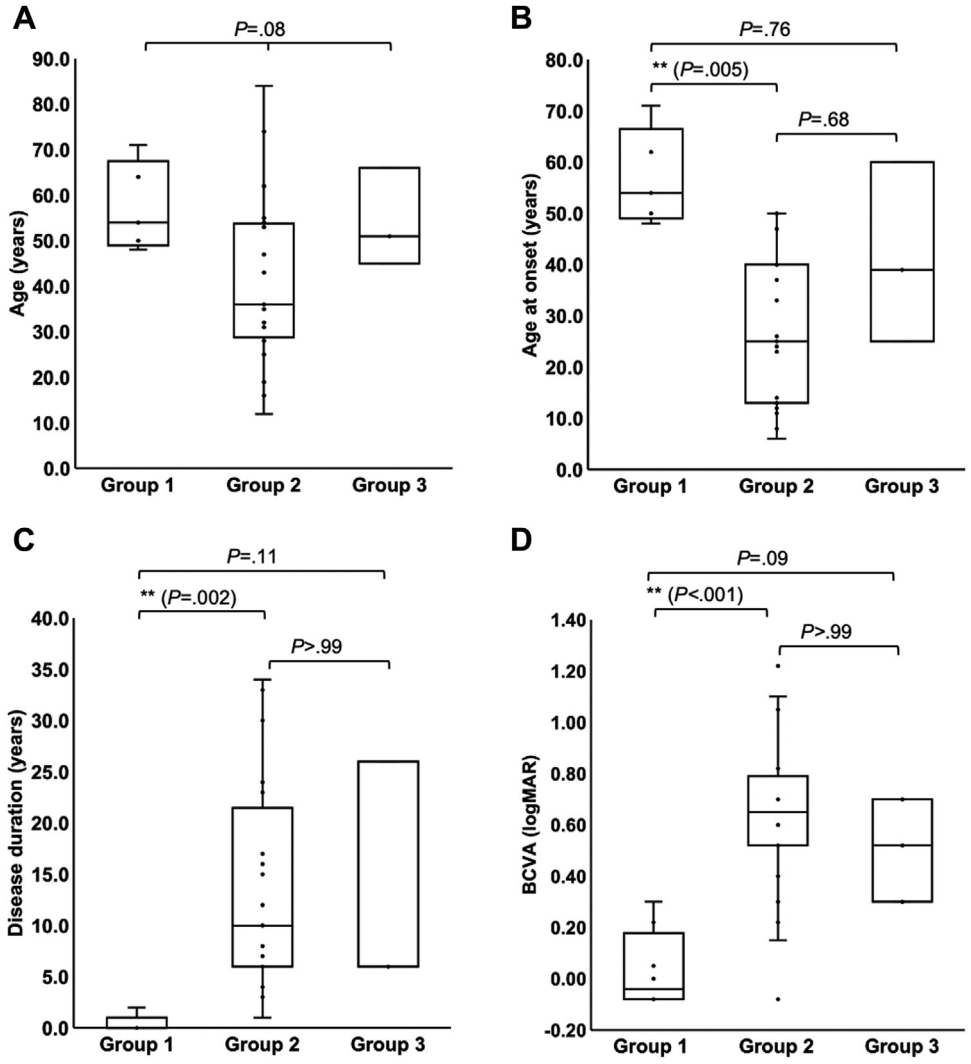

FIGURE 3. Clinical parameters for 3 functional groups. The ends of the boxes represent the upper and lower quartiles. The middle line in the box is the median value. Maximum and minimum values are shown as the upper and lower ends of the whiskers. (A) Age. There was no significant difference between the groups (95% confidence interval [CI] for Groups 1, 2, 3: 45.2 to 69.5, 32.2 to 49.8, 27.1 to 80.9, respectively; $P = .08$). (B) Age at disease onset. There was a significant difference between Groups 1 and 2 (95% CI, 45.2 to 68.8 and 20.3 to 34.4, respectively; $P = .005$), with no significant difference between Groups 1 and 3 (95% CI, 45.2 to 68.8 and −2.4 to 85.1, respectively; $P = .76$) or Groups 2 and 3 (95% CI, 20.3 to 34.4 and −2.4 to 85.1, respectively; $P = .68$). (C) Disease duration. There was a significant difference between Groups 1 and 2 in disease duration (95% CI, −0.7 to 1.5 and 8.9 to 18.4, respectively; $P = .002$), with no significant difference between Groups 1 and 3 (95% CI, −0.7 to 1.5 and −16.0 to 41.4, respectively; $P = .11$) or Groups 2 and 3 (95% CI, 8.9 to 18.4 and −16.0 to 41.4; $P > .99$). (D) Best-corrected visual acuity (BCVA) (converted to logMAR). There was a significant difference between Groups 1 and 2 (95% CI, −0.09 to 0.16 and 0.52 to 0.69, respectively; $P < .001$), with no significant difference between Groups 1 and 3 (95% CI, −0.09 to 0.16 and 0.26 to 0.75, respectively; $P = .09$) or Groups 2 and 3 (95% CI, 0.52 to 0.69 and 0.26 to 0.75, respectively; $P > .99$).

parafovea was first identified in the current study. The functional/structural damages in the parafovea were found correspondently in our cohort, although further detailed analysis in the natural course is required to reveal which of function and structure is impaired earlier. Interestingly, similar patterns were also found in other macular dystrophies or cone/cone-rod dystrophies—for example, *ABCA4*-associated, *POC1B*-associated, *CRX*-associated, and *GUCY2D*-associated retinal disorders.[27,31–35] However, the underlying mechanism to explain this phenotype of preceding parafoveal changes is still uncertain. Thus, the possibility of a particular phase of disease severity showing the aforementioned distinct mild features that progress to widespread dysfunction has not been fully excluded. Some of the clinical features were shared between the 2 subgroups of patients demonstrating

TABLE 4. Distribution of Functional Groups and Morphologic Subtypes

mfERG Functional Group[a]	SDOCT Classification[b]		
	Mild Phenotype	Severe Phenotype	Total Number
Group 1	8	0	8
Group 2	2	38	40
Group 3	0	5	5

mfERG = multifocal electroretinogram; SDOCT = spectral-domain optical coherence tomography.

Number of eyes are shown.

γ=1.00; $P < .001$. Goodman-Kruskal gamma.

[a]All eyes were classified into 3 mfERG functional groups: Group 1 - paracentral dysfunction; Group 2 - homogeneous central/paracentral dysfunction with preserved peripheral function; and Group 3 - widespread dysfunction over the whole area tested.

[b]All eyes were classified into 2 subtypes based on SDOCT findings; (1) severe phenotype, showing both blurred/flat ellipsoid zone (EZ) and absence of interdigitation zone (IZ); and (2) mild phenotype, defined as minimum/local blurring of EZ and local absence of IZ.

homogeneous central dysfunction with preserved peripheral function (Group 2) and widespread dysfunction (Group 3), including age at onset, BCVA, and frequently found blurred/flat EZ. Notably, patients with intermediate and severe BCVA had decreased mfERG ratio (R1/R5) in the central retina, which implies that the objective functional impairment could precede the subjective functional impairment of visual acuity in the central retina in these patients. These features suggest that the extent of retinal dysfunction or the degree of severity can vary in Miyake disease.

There are limitations in this study. A challenge for this multicenter international study was that 5 different mfERG recording protocols were used in different laboratories. Thus, it is difficult to statistically perform the comparison data analysis directly with absolute values of mfERG. Also, the statistical comparison analysis between normative control and patients with Miyake disease was not available, owing to the relatively wide range of normal values, as well as the limited sample number of some recording protocols. However, all 3 centers established the same underlying functional phenotype, facilitated by use of the standard ISCEV mfERG protocol and enabling pooling of data and resources.[14] Quantitative differences were anticipated in the ring ratio analysis of mfERGs, given the different number of rings associated with different mfERG instruments. It is recognized that a limitation of the mfERG ring analysis was that patients in Group 3 had abnormal peripheral (R5/R6) responses, confounding direct comparison of ring ratios with patients in Groups 1 and 2 (with preserved peripheral responses). The cross-sectional data described above suggest the possibility of progressive dysfunction and expanding maculopathy, but longitudinal monitoring will be required to investigate the stability of the milder phenotypes. To prove the hypothesis that the functional groups might be related to the natural course of OMD, a long-term follow-up study is needed in the future. Additional studies based on a larger cohort could help to further elucidate the underlying disease mechanism of Miyake disease by clarifying genotype-phenotype associations.

In conclusion, the current multicenter study expands the spectrum of functional phenotypes of Miyake disease, which is useful for the diagnosis, classification, and prediction of disease progression. Our detailed assessment of spatial tendency using ring ratio analyses illustrated 3 functional phenotypes representing circular functional damage: paracentral dysfunction, homogeneous central dysfunction, and widespread dysfunction. Patients with paracentral dysfunction had milder phenotypes; meanwhile, patients with homogeneous central dysfunction and widespread dysfunction showed overlapping phenotypes, suggesting the various extents of retinal dysfunction.

FUNDING/SUPPORT: THE EAOMD STUDIES ARE SUPPORTED BY A GRANT-IN-AID FOR YOUNG SCIENTISTS (A) OF THE MINISTRY of Education, Culture, Sports, Science and Technology, Japan (16H06269); and Grant-in-Aid for Scientists to support international collaborative studies of the Ministry of Education, Culture, Sports, Science and Technology, Japan (16KK01930002). The authors also indicate the following support: Kazushige Tsunoda: Support–Japan Agency for Medical Research and Development, the Ministry of Health, Labor and Welfare, Japan (18ek0109282h0002); Grants–for Scientific Research, Japan Society for the Promotion of Science, Japan (H26-26462674). Yu Fujinami-Yokokawa: Grants–Grant-in-Aid for Young Scientists of the Ministry of Education, Culture, Sports, Science and Technology, Japan (18K16943). Gavin Arno: Support–Fight for Sight (UK) Early Career Investigator award, NIHR-BRC at Moorfields Eye Hospital and the UCL Institute of Ophthalmology, and Great Britain Sasakawa Foundation Butterfield Award, UK. Anthony G. Robson: Support–is supported by the NIHR Biomedical Research Centre at Moorfields Eye Hospital NHS Foundation Trust and UCL Institute of Ophthalmology and by the Moorfields Eye Charity. Toshihide Kurihara: Support–Tsubota Laboratory, Inc, Fuji Xerox Co, Ltd, Kirin Company, Ltd, Kowa Company, Ltd, Novartis Pharmaceuticals, Santen Pharmaceutical Co, Ltd, ROHTO Pharmaceutical Co, Ltd. Takeshi Iwata: Support–AMED (18ek0109282h0002). Se Joon Woo: Grants–Seoul National University Bundang Hospital (16-2019-003), National Research Foundation of Korea grant 2016R1D1A1B03934724, funded by the Korean government (Ministry of Science, ICT and Future Planning [MSIP]). Ruifang Sui: Grants–Foundation Fighting Blindness (CD-CL-0214-0631-PUMCH); CAMS Innovation Fund for Medical Sciences, China, CIFMS 2016-12M-1-002; National Natural Science Foundation of China, China, 81873687. Kaoru Fujinami: Grants - Grant-in-Aid for Young Scientists (A) of the Ministry of Education, Culture, Sports, Science and Technology, Japan (16H06269); Grant-in-Aid for Scientists to support international collaborative studies of the Ministry of Education, Culture, Sports, Science and Technology, Japan (16KK01930002); National Hospital Organization Network Research Fund, Japan (H30-NHO-Sensory Organs-03); AMED (18ek0109355h0001); Foundation Fighting Blindness Alan Laties Career Development Program (CF-CL-0416-0696-UCL), USA; Health Labour Sciences Research Grant, The Ministry of Health Labour and Welfare, Japan (201711107A);

Great Britain Sasakawa Foundation Butterfield Awards, UK. Role of the Funder/Sponsor: the sponsor or funding organization had no role in the design or conduct of this research. Financial Disclosures: The individual investigators who participate in the sponsored project(s) are not directly compensated by the sponsor but may receive salary or other support from the institution to support their effort on the project(s). Kaoru Fujinami has the following disclosures: Paid consultant–Astellas Pharma Inc, Kubota Pharmaceutical Holdings Co, Ltd, Acucela Inc, Novartis AG, Janssen Pharmaceutica, Sanofi Genzyme, NightstaRx Limited; Personal fees–Astellas Pharma Inc, Kubota Pharmaceutical Holdings Co, Ltd, Acucela Inc, Novartis AG, Santen Company Limited, Foundation Fighting Blindness, Foundation Fighting Blindness Clinical Research Institute, Japanese Ophthalmology Society, Japan Retinitis Pigmentosa Society; Grants–Astellas Pharma Inc. (NCT03281005), outside the submitted work. Se Joon Woo has the following disclosures: Paid consultant–Samsung Bioepis Inc., Panolos Bioscience Inc., Novelty Nobility Inc.; Co-founder of Retimark Inc., outside the submitted work. The following authors have no financial disclosures: Lizhu Yang, Kwangsic Joo, Kazushige Tsunoda, Mineo Kondo, Yu Fujinami-Yokokawa, Gavin Arno, Nikolas Pontikos, Xiao Liu, Natsuko Nakamura, Toshihide Kurihara, Kazuo Tsubota, Takeshi Iwata, Hui Li, Xuan Zou, Shijing Wu, Zixi Sun, Seong Joon Ahn, Min Seok Kim, Yong Seok Mun, Kyu Hyung Park, Anthony G. Robson, Yozo Miyake, Ruifang Sui. All authors attest that they meet the current ICMJE criteria for authorship.

Acknowledgment: This international multicenter study conducted by the East Asia Inherited Retinal Disease Society has been performed in 3 countries: Japan, China, and South Korea. Owing to the private information protection laws in each country, some data (such as deep genetic data or detailed clinical data) are not allowed to be shared across borders. The 3 corresponding authors from each country therefore have full data access separately in their home countries and take responsibility for the integrity of the data and the accuracy of the data analysis. The private information protection laws of China, Korea, and Japan for bioresources do not allow us to present/publish the genetic/clinical data of patients from their own countries without the corresponding local author taking clear responsibility.

Acknowledgment: The authors thank the patients and their families for the participation in this study, as well as all the collaborators of East Asia Inherited Retinal Disease Society (https://www.fujinamik.com/east-asia-inherited-retinal-disease) and Japan Eye Genetics Consortium (http://www.jegc.org/) for data collection.

The East Asia Inherited Retinal Disease Society (EAIRDs) Study Group: The EAOMD study is supported by a contract from the EAIRDs. The EAIRDs Study Group members are as follows: Chair's Office: National Institute of Sensory Organs, Kaoru Fujinami, Se Joon Woo, Ruifang Sui, Shiying Li, Hyeong Gon Yu, Bo Lei, Qingjiong Zhang, Chan Choi Mun, Fred Chen, Takeshi Iwata, Kazushige Tsunoda, Yozo Miyake, Mineo Kondo, Kunihiko Akiyama, Gen Hanazono, Masaki Fukui, Yu Fujinami-Yokokawa, Takayuki Kinoshita, Tatsuo Matsunaga, Satomi Inoue, Kazuki Yamazawa, Yasuiro Yamada, Michel Michaelides, Gavin Arno, Nikolas Pontikos, Yasutaka Suzuki, Asako Ihama, Reina Akita, Jun Ohashi, Izumi Naka, Kazutoshi Yoshitake, Daisuke Mori, Toshihide Kurihara, Kazuo Tsubota, Hiroaki Miyata, Kei Shinoda, Atsushi Mizota, Natsuko Nakamura, Takaaki Hayashi, Kazuki Kuniyoshi, Shuhei Kameya, Yusuke Murakami, Kwangsic Joo, Min Seok Kim, Kyu Hyung Park, Seong Joon Ahn, Dae Joong Ma, Joo Yong Lee, Sang Jin Kim, Christopher Seungkyu Lee, Jinu Han, Hyewon Chung, Jeeyun Ahn, Min Sagong, Young-Hoon-Ohn, Dong Ho Park, You Na Kim, Jong Suk Lee, Sang Jun Park, Jun Young Park, Won Kyung Song, Tae Kwan Park, Baek-Lok Oh, Jong Young Lee, Lizhu Yang, Xuan Zou, Hui Li, Zhengqin Yin, Yong Liu, Xiaohong Meng, Xiao Liu, Yanling Long, Jiayun Ren, Hongxuan Lie, Gang Wang, Anthony G. Robson, Xuemin Jin, Kunpeng Xie, Ya Li, Chonglin Chen, Qingge Guo, Lin Yang, Ya You, Tin Aung, Graham E. Holder.

REFERENCES

1. Miyake Y, Ichikawa K, Shiose Y, Kawase Y. Hereditary macular dystrophy without visible fundus abnormality. *Am J Ophthalmol* 1989;108(3):292–299.
2. Miyake Y, Horiguchi M, Tomita N, et al. Occult macular dystrophy. *Am J Ophthalmol* 1996;122(5):644–653.
3. Miyake Y, Tsunoda K. Occult macular dystrophy. *Jpn J Ophthalmol* 2015;59(2):71–80.
4. Fujinami K, Yang L, Joo K, et al. Clinical and genetic characteristics of East Asian patients with occult macular dystrophy (Miyake Disease): East Asia Occult Macular Dystrophy Studies Report Number 1. *Ophthalmology* 2019;126(10):1432–1444.
5. Akahori M, Tsunoda K, Miyake Y, et al. Dominant mutations in RP1L1 are responsible for occult macular dystrophy. *Am J Hum Genet* 2010;87(3):424–429.
6. Tsunoda K, Usui T, Hatase T, et al. Clinical characteristics of occult macular dystrophy in family with mutation of RP1l1 gene. *Retina* 2012;32(6):1135–1147.
7. Fujinami K, Kameya S, Kikuchi S, et al. Novel RP1L1 variants and genotype-photoreceptor microstructural phenotype associations in cohort of Japanese patients with occult macular dystrophy. *Invest Ophthalmol Vis Sci* 2016;57(11):4837–4846.
8. Fujii S, Escano MF, Ishibashi K, Matsuo H, Yamamoto M. Multifocal electroretinography in patients with occult macular dystrophy. *Br J Ophthalmol* 1999;83(7):879–880.
9. Piao CH, Kondo M, Tanikawa A, Terasaki H, Miyake Y. Multifocal electroretinogram in occult macular dystrophy. *Invest Ophthalmol Vis Sci* 2000;41(2):513–517.
10. Wildberger H, Niemeyer G, Junghardt A. Multifocal electroretinogram (mfERG) in a family with occult macular dystrophy (OMD). *Klin Monbl Augenheilkd* 2003;220(3):111–115.
11. Kabuto T, Takahashi H, Goto-Fukuura Y, et al. A new mutation in the RP1L1 gene in a patient with occult macular dystrophy associated with a depolarizing pattern of focal macular electroretinograms. *Mol Vis* 2012;18:1031–1039.
12. Hanazono G, Ohde H, Shinoda K, Tsunoda K, Tsubota K, Miyake Y. Pattern-reversal visual-evoked potential in patients with occult macular dystrophy. *Clin Ophthalmol* 2010;4:1515–1520.
13. Davidson AE, Sergouniotis PI, Mackay DS, et al. RP1L1 variants are associated with a spectrum of inherited retinal diseases including retinitis pigmentosa and occult macular dystrophy. *Hum Mutat* 2013;34(3):506–514.
14. Hood DC, Bach M, Brigell M, et al. ISCEV standard for clinical multifocal electroretinography (mfERG) (2011 edition). *Doc Ophthalmol* 2012;124(1):1–13.
15. Robson AG, Nilsson J, Li S, et al. ISCEV guide to visual electrodiagnostic procedures. *Doc Ophthalmol* 2018;136(1):1–26.
16. Ahn SJ, Cho SI, Ahn J, Park SS, Park KH, Woo SJ. Clinical and genetic characteristics of Korean occult macular dystrophy patients. *Invest Ophthalmol Vis Sci* 2013;54(7):4856–4863.
17. Fujinami K, Tsunoda K, Hanazono G, Shinoda K, Ohde H, Miyake Y. Fundus autofluorescence in autosomal dominant occult macular dystrophy. *Arch Ophthalmol* 2011;129(5):597–602.
18. Ahn SJ, Ahn J, Park KH, Woo SJ. Multimodal imaging of occult macular dystrophy. *JAMA Ophthalmol* 2013;131(7):880–890.

19. Kato Y, Hanazono G, Fujinami K, et al. Parafoveal photoreceptor abnormalities in asymptomatic patients with RP1L1 mutations in families with occult macular dystrophy. *Invest Ophthalmol Vis Sci* 2017;58(14):6020–6029.
20. Zobor D, Zobor G, Hipp S, et al. Phenotype variations caused by mutations in the RP1L1 gene in a large mainly German cohort. *Invest Ophthalmol Vis Sci* 2018;59(7):3041–3052.
21. Nakamura N, Tsunoda K, Mizuno Y, et al. Clinical stages of occult macular dystrophy based on optical coherence tomographic findings. *Invest Ophthalmol Vis Sci* 2019;60(14):4691–4700.
22. Nakanishi A, Ueno S, Kawano K, et al. Pathologic changes of cone photoreceptors in eyes with occult macular dystrophy. *Invest Ophthalmol Vis Sci* 2015;56(12):7243–7249.
23. Hayashi T, Gekka T, Kozaki K, et al. Autosomal dominant occult macular dystrophy with an RP1L1 mutation (R45W). *Optom Vis Sci* 2012;89(5):684–691.
24. Kitaguchi Y, Kusaka S, Yamaguchi T, Mihashi T, Fujikado T. Detection of photoreceptor disruption by adaptive optics fundus imaging and Fourier-domain optical coherence tomography in eyes with occult macular dystrophy. *Clin Ophthalmol* 2011;5:345–351.
25. Fujinami-Yokokawa Y, Pontikos N, Yang L, et al. Prediction of causative genes in inherited retinal disorders from spectral-domain optical coherence tomography utilizing deep learning techniques. *J Ophthalmol* 2019;2019:1691064.
26. Park SJ, Woo SJ, Park KH, Hwang JM, Chung H. Morphologic photoreceptor abnormality in occult macular dystrophy on spectral-domain optical coherence tomography. *Invest Ophthalmol Vis Sci* 2010;51(7):3673–3679.
27. Kameya S, Fujinami K, Ueno S, et al. Phenotypical characteristics of POC1B-associated retinopathy in Japanese cohort: cone dystrophy with normal funduscopic appearance. *Invest Ophthalmol Vis Sci* 2019;60(10):3432–3446.
28. Wang F, Wang H, Tuan HF, et al. Next generation sequencing-based molecular diagnosis of retinitis pigmentosa: identification of a novel genotype-phenotype correlation and clinical refinements. *Hum Genet* 2014;133(3):331–345.
29. Sun Z, Zhou Q, Li H, Yang L, Wu S, Sui R. Mutations in crystallin genes result in congenital cataract associated with other ocular abnormalities. *Mol Vis* 2017;23:977–986.
30. Yuan Z, Li B, Xu M, et al. The phenotypic variability of HK1-associated retinal dystrophy. *Sci Rep* 2017;7(1):7051.
31. Fujinami K, Lois N, Mukherjee R, et al. A longitudinal study of Stargardt disease: quantitative assessment of fundus autofluorescence, progression, and genotype correlations. *Invest Ophthalmol Vis Sci* 2013;54(13):8181–8190.
32. Khan KN, Kasilian M, Mahroo OAR, et al. Early patterns of macular degeneration in ABCA4-associated retinopathy. *Ophthalmology* 2018;125(5):735–746.
33. Fujinami K, Sergouniotis PI, Davidson AE, et al. Clinical and molecular analysis of Stargardt disease with preserved foveal structure and function. *Am J Ophthalmol* 2013;156(3):487–501.e1.
34. Fujinami-Yokokawa Y, Fujinami K, Kuniyoshi K, et al. Clinical and genetic characteristics of 18 patients from 13 Japanese families with CRX-associated retinal disorder: identification of genotype-phenotype association. *Sci Rep* 2020;10(1):9531.
35. Liu X, Fujinami K, Kuniyoshi K, et al. Clinical and genetic characteristics of 15 affected patients from 12 Japanese families with GUCY2D-associated retinal disorder. *Transl Vis Sci Technol* 2020;9(6):2.